Dynamic collision frequency for a two-component plasma

2003 J. Phys. A: Math. Gen. 36 6259

(http://iopscience.iop.org/0305-4470/36/22/356)

INSTITUTE OF PHYSICS PUBLISHING JOURNAL OF PHYSICS A: MATHEMATICAL AND GENERAL

J. Phys. A: Math. Gen. **36** (2003) 6259–6264 PII: S0305-4470(03)54741-2

Dynamic collision frequency for a two-component plasma

Th Millat[1], A Selchow[1], A Wierling[2], H Reinholz[3], R Redmer[1] and G Röpke[1]

[1] Department of Physics, University of Rostock, 18051 Rostock, Germany
[2] Department of Fundamental Energy Science, Kyoto University, Uji, Kyoto 611-0011, Japan
[3] School of Physics, The University of Western Australia, Nedlands, WA 6907, Australia

E-mail: thomas.millat@physik.uni-rostock.de

Received 12 October 2002, in final form 29 January 2003
Published 22 May 2003
Online at stacks.iop.org/JPhysA/36/6259

Abstract

Starting from a generalized response theory, the inverse response function can be expressed in terms of equilibrium correlation functions for which a perturbation expansion is carried out. In the long-wavelength limit, this can be exploited to obtain an approximation for the dynamic collision frequency. Utilizing the Mermin ansatz, the dynamical structure factor is determined from the long-wavelength limit. The results are compared with classical simulation data. Different effective potentials which model the electron–ion interaction are discussed. It is shown that the high-frequency behaviour of the dynamic collision frequency is sensitive to the form of the chosen interaction.

PACS numbers: 52.25.Mq, 52.27.Gr, 52.38.−r, 52.38.Dx

1. Dielectric function and dynamic collision frequency

The dielectric function $\epsilon(\vec{k},\omega)$ describing the response of a charged many particle system to an external, time- and space-dependent electric field is related to various phenomena such as optical absorption of light, collective excitations, dynamic screening, compressibility, dynamic structure factor, dynamic electrical conductivity and diffusion. The dielectric function

$$\epsilon(\vec{k},\omega) = 1 - \frac{\Pi(\vec{k},\omega)}{\epsilon_0 k^2} = 1 + \frac{\mathrm{i}\sigma(\vec{k},\omega)}{\epsilon_0\omega} = \frac{1}{1+\chi(\vec{k},\omega)/(\epsilon_0 k^2)} \tag{1}$$

can be expressed in terms of the polarization function $\Pi(\vec{k},\omega)$ or in terms of the response function $\chi(\vec{k},\omega)$. It is related to the dynamic electrical conductivity $\sigma(\vec{k},\omega)$ via Ampere's law. The response function

$$\chi(\vec{k},\omega) = \mathrm{i}\beta\Omega_0 \frac{k^2}{\omega}\frac{1}{M(\vec{k},\omega)} \tag{2}$$

is connected to an inverse response function $M(\vec{k},\omega)$, which can be expressed in terms of equilibrium correlation functions [1] allowing for a systematic evaluation within a perturbation theory [2, 3][1]. Although the response function $M(\vec{k},\omega)$ can be evaluated at arbitrary values of k, the calculation is tedious. Instead, we perform a perturbative evaluation in the long-wavelength limit and use the Mermin approach [8] to obtain values for χ at finite k. The dynamic collision frequency $\nu(\omega)$ can be introduced taking the long-wavelength limit $k\to 0$ of the dielectric function leading to a generalized Drude formula [4]

$$\epsilon(\omega) = 1 - \frac{\omega_{\rm pl}^2}{\omega(\omega + {\rm i}\nu(\omega))} \tag{3}$$

where the dynamic collision frequency is given as

$$\nu(\omega) = -\frac{\epsilon_0\omega_{\rm pl}^2}{\beta\Omega_0}\lim_{k\to 0} M(\vec{k},\omega) + {\rm i}\omega\left(1 - \frac{\omega_{\rm pl}^2}{\omega^2}\right). \tag{4}$$

According to (1), the dynamic conductivity $\sigma(\omega) = {\rm i}\epsilon_0\omega_{\rm pl}^2/[\omega + {\rm i}\nu(\omega)]$ can be obtained from the collision frequency. For further analysis, we consider a fully ionized hydrogen plasma $\left(n_e = n_i, e_e^2 = e_i^2 = e^2\right)$ in adiabatic limit $m_i/m_e \to \infty$.

In a one-moment approach we use the electrical current–density $\vec{J}_k^{\rm el} = \Omega_0^{-1}\sum_{c,p} e_c/m_c\hbar\vec{p}n_{p,k}^c$, where $c = e, i$, as a relevant observable, see [4]. After performing an expansion of the inverse response function with respect to the interaction, the collision frequency is obtained from a force–force correlation function according to

$$\nu(\omega) = \frac{\beta\Omega_0}{\epsilon_0\omega_{\rm pl}^2}\left\langle\vec{J}_0^{\rm el};\, \vec{J}_0^{\rm el}\right\rangle_{\omega+{\rm i}\eta}^{\rm irred}. \tag{5}$$

The force–force correlation $\left\langle\vec{J}_0^{\rm el};\, \vec{J}_0^{\rm el}\right\rangle_{\omega+{\rm i}\eta}^{\rm irred}$ (see footnote 2) itself can be expressed in terms of the interaction potential, which is equivalent to a four-particle Green function $G(\omega)$. The correlation function is defined as

$$\langle A;\, B\rangle_z = \frac{\rm i}{\beta Z}\int_0^\infty {\rm d}t\, {\rm e}^{{\rm i}zt}\int_0^\beta {\rm d}\tau\, {\rm Tr}[\rho_0 A(t - {\rm i}\hbar\tau)B^\dagger] \tag{6}$$

where ρ_0 is the equilibrium statistical operator and Z is the partition function, for details see [4]. Thus, the technique of thermodynamic Green functions can be used to perform a systematic perturbative treatment of the collision frequency for non-ideal plasmas. Performing partial summations, the Green function was evaluated in different approximations, see [4, 5], e.g., considering the effects of static screened interaction $\nu^{\rm Born,s}(\omega)$, dynamically screened interaction $\nu^{\rm LB}(\omega)$ and strong collisions (T-matrix) $\nu^{\rm T,s}(\omega)$, treated in a static approximation. As an example, the collision frequency accounting for dynamic screening of the potential $V_{ei}(q)$ is quoted here

$$\nu^{\rm LB}(\omega) = {\rm i}\frac{\epsilon_0\Omega_0^2}{6\pi^2 e^2 m_e}\int_0^\infty {\rm d}q\, q^6 V_{ei}^2(q)\frac{\epsilon_{\rm RPA}^{-1}(q,\omega) - \epsilon_{\rm RPA}^{-1}(q,0)}{\omega}. \tag{7}$$

The quantity $\epsilon_{\rm RPA}(q,\omega)$ denotes the dielectric function in random phase approximation (RPA). Due to momentum conservation, there is no contribution from the interaction between particles of the same species in this one-moment approach.

Following an approach by Gould and DeWitt [6], dynamical screening and strong collisions are accounted for by an interpolation scheme [5]

$$\nu \approx \nu^{\rm Born,s} + (\nu^{\rm T,s} - \nu^{\rm Born,s}) + (\nu^{\rm LB} - \nu^{\rm Born,s}). \tag{8}$$

[1] Ω_0 is the normalization volume.

[2] The index irred indicates that only those diagrams contribute to the correlation function, which cannot be separated into two pieces by cutting a single interaction line.

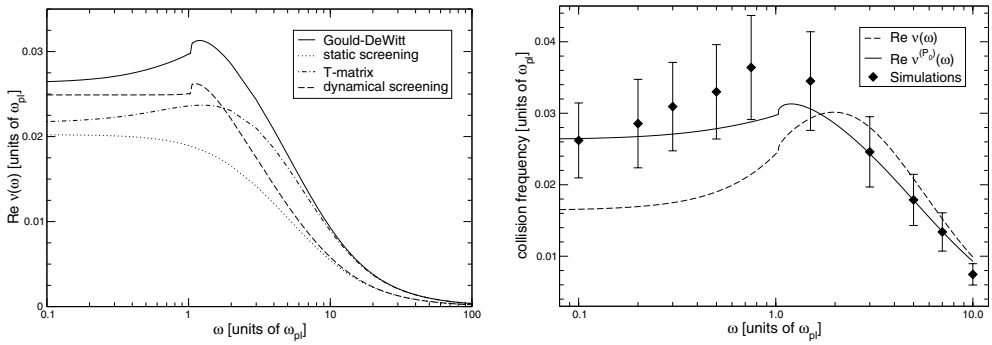

Figure 1. Left: frequency dependence of the real part of the collision frequency $\nu(\omega)$ for a hydrogen plasma with $n = 1.51 \times 10^{25}\,\mathrm{cm}^{-3}$ and $T = 573$ eV corresponding to $\Gamma = 0.1$. Different approximations [5] are compared. Right: dynamical collision frequency $\nu(\omega)$ modified by the renormalization factor compared to the unrenormalized collision frequency $\nu^{(P_0)}(\omega)$ and numerical simulations, according to the approach in [7].

In this way, the leading order of the collision frequency is dynamically screened, whereas higher diagrams are statically screened. The approximations are compared in figure 1. As can be seen from the figure, the dynamic and static screening results almost coincide with the high-frequency limit. In this way, the Gould–DeWitt result is dominated by the contribution from strong collisions. The peak in the dynamic screening result close to the plasma frequency is due to the emergence of plasmon excitations. It is modified, if scattering is taken into account.

Electron–electron collisions can be integrated into our approach by inclusion of higher moments. These effects give rise to a frequency-dependent renormalization factor [4]. A multiplication of the one-moment result by the renormalization factor leads to a dynamic collision frequency reproducing the correct static limit and dc conductivity. In figure 1, the real part of the modified collision frequency is compared to molecular dynamics (MD) simulation data. These have been calculated using a code by Pfalzner and Gibbon [7]. For low frequencies, the renormalized collision frequency is decreased compared to the unmodified one, while for frequencies higher than about ω_{pl}, the collision frequency is increased. The perturbative results are consistent with the MD data for large frequencies whereas discrepancies arise at small frequencies. It should be noted that the theoretical results are obtained by a quantum mechanical calculation using the Coulomb interaction, while the simulation data are obtained by a classical simulation [7] with a soft-core potential discussed in the next section.

The calculation of the collision frequency can be extended to finite wave vectors k. However, to avoid tedious calculations, the structure factor at finite k is calculated with a generalized Mermin ansatz [8] using the dynamic collision frequency (7) instead of a frequency-independent relaxation time τ. The response function is given by

$$\chi(k,\omega) = \left(1 - \frac{\mathrm{i}\omega}{\nu(\omega)}\right) \frac{\chi^0(k,\omega + \mathrm{i}\nu(\omega))\chi^0(k,0)}{\chi^0(k,\omega+\mathrm{i}\nu(\omega)) - \mathrm{i}\omega/\nu(\omega)\chi^0(k,0)} \tag{9}$$

where $\chi^0(k,z)$ represents the RPA susceptibility. As shown in [10], the Mermin ansatz can be derived within the framework of the generalized linear response theory. It fulfils first-order sum rules and reproduces the generalized Drude response function in the long-wavelength limit. Thus, it is a consistent ansatz to extrapolate results obtained at $k \to 0$ to finite k.

Table 1. Effective potentials.

Deutsch-like [11]	Soft-core [7]	Error function [12]
$V_{cd}^{\mathrm{D}}(r) = \frac{e_c e_d}{4\pi\epsilon_0\Omega_0}\frac{1-\exp(-r/\Lambda_{cd})}{r}$	$V_{cd}^{\mathrm{S}}(r) = \frac{e_c e_d}{4\pi\epsilon_0\Omega_0}\frac{1}{(r^2+\Lambda_{cd}^2)^{1/2}}$	$V_{cd}^{\mathrm{E}}(r) = \frac{e_c e_d}{4\pi\epsilon_0\Omega_0}\frac{1}{r}\mathrm{Erf}(\frac{r}{\Lambda_{cd}})$

2. Effective potentials

Performing MD simulations, it is necessary to introduce a quasi-classical effective interaction instead of the Coulomb interaction to avoid the Coulomb-implosion and to model quantum effects. For a comparison of theoretical results and simulation, it is essential to calculate the considered quantities on the same level of approximation and with the same interaction potential. Thus, we also introduce effective potentials in our theoretical approach. Some often used effective potentials are shown in table 1. These potentials have no singularity at the origin (soft-core potentials) and reproduce the Coulomb potential for large distances. The behaviour for small distances is determined by the free parameter Λ_{cd} which has to be chosen in a proper way, e.g., as a thermal wavelength, in order to mimic quantum effects.

Using these effective interactions, a dynamic collision frequency $\nu(\omega)$ can be calculated in the same way as before. Some qualitative properties of the dynamic collision frequency, for instance, the peak in the dynamically screened result, remain unaffected by the choice of the potential. Although the potentials show similar characteristics (see figure 2), the asymptotic behaviour of the dynamic collision frequency varies strongly. An analysis of (7) for the high-frequency asymptote leads for a Deutsch-like potential to

$$\nu_{\mathrm{D}}(\omega \to \infty) \sim \frac{1}{\Lambda_{cd}^4(\hbar\omega)^{7/2}} \tag{10}$$

for a soft-core potential to

$$\nu_{\mathrm{S}}(\omega \to \infty) \sim \frac{\Lambda_{cd}}{(\hbar\omega)^{3/2}}\exp\left\{-\Lambda_{cd}\sqrt{\frac{8m_e\omega}{\hbar}}\right\} \tag{11}$$

and using the error function potential to

$$\nu_{\mathrm{E}}(\omega \to \infty) \sim \frac{1}{\sqrt{a}(\hbar\omega)^{3/2}}\exp\left\{-\frac{\hbar\omega}{2k_{\mathrm{B}}T}(a-1)\right\} \qquad a = \sqrt{1+\frac{4k_{\mathrm{B}}Tm_e}{\hbar^2}\Lambda_{cd}^2}. \tag{12}$$

For comparison, the asymptotic behaviour using the Coulomb potential is proportional to $(\hbar\omega)^{-3/2}$. The numerical results for the dynamically screened collision frequency (7) applying effective interactions and the respective asymptotes are shown in figure 2. The collision frequencies show a strongly varying high-frequency behaviour in agreement with the analytic asymptotes.

Furthermore, the free parameter Λ_{cd} affects the collision frequency. The smaller this parameter the greater the dynamic collision frequency. In the limit $\Lambda_{cd} \to 0$, which has to be calculated before executing the frequency limit, the collision frequency for the Coulomb potential is reproduced.

3. Dynamic structure factor: comparison with simulation

The fluctuation dissipation theorem, here in the classical limit,

$$S(k,\omega) = -\frac{k_{\mathrm{B}}T}{n\omega}\,\mathrm{Im}\,\chi(k,\omega) = -\frac{\epsilon_0 k_{\mathrm{B}}T}{n}\frac{k^2}{\omega}\,\mathrm{Im}\,\epsilon^{-1}(k,\omega) \tag{13}$$

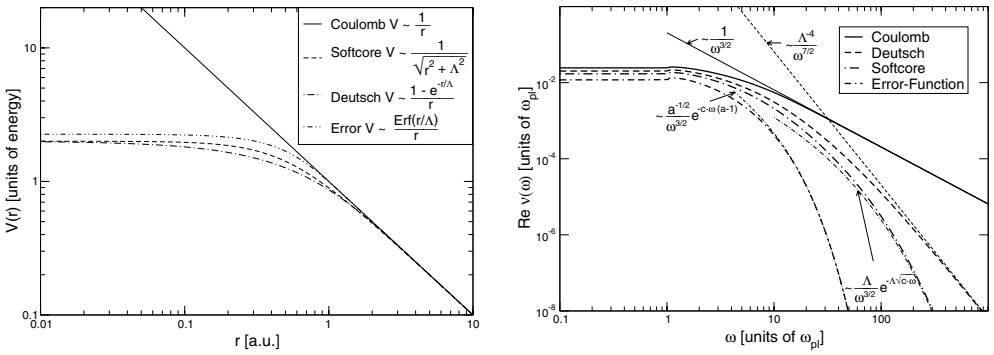

Figure 2. Left: comparison of Coulomb potential and some quasi-classical effective potentials used in simulations. Right: frequency dependence of the real part of the collision frequency $\nu(\omega)$ (7) for different dynamical screened potentials. Parameters are the same as in figure 1. For comparison, the respective asymptotes are shown as thin lines.

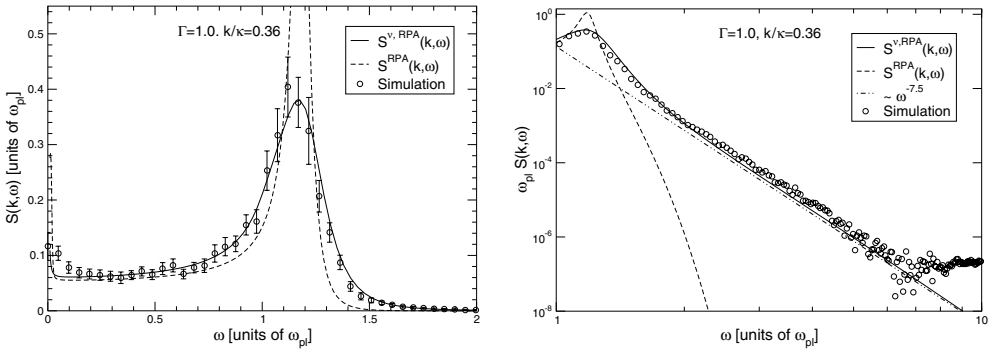

Figure 3. Left: dynamic structure factor $S(k,\omega)$ for an electron–proton model plasma with a Deutsch-like effective interaction in RPA (dashed line) and in Mermin-like approximation which utilizes a dynamically screened collision frequency $\nu^{\Lambda,\mathrm{RPA}}(\omega)$ [9] (solid line). Note that the RPA approximation does not reproduce the simulation data. Accounting for dynamic screening in the collision frequency is essential for a reasonable agreement. Right: log–log plot of the dynamic structure factor. In the high-frequency limit, a $1/\omega^{7.5}$ asymptote is predicted for a two-component plasma with a Deutsch-like effective potential. For comparison, this asymptote is shown as dashed–dotted line.

relates the imaginary part of the density response function (2) to the dynamic structure factor $S(k,\omega)$ [13]. Thus, we can compare our results with classical MD simulations for the dynamic structure factor of a two-component plasma-like system calculated by Zwicknagel [14]. In their MD simulations a Deutsch-like effective interaction (table 1) is used. Using the Mermin ansatz (9) and the collision frequency (7), we are able to calculate a dynamic structure factor for given plasma conditions and wave vectors [8]. A comparison of our theoretical results with the simulation results shows a good agreement, see figure 3.

An objective of this work is the study of the high-frequency behaviour of the structure factor. Using the high-frequency expansion for the inverse of the dielectric function (3) we obtain

$$S(k,\omega\to\infty) \approx \frac{k_\mathrm{B}T}{m_e}k^2\frac{\mathrm{Re}\,\nu(\omega)}{\omega^4} \tag{14}$$

for the asymptotic behaviour. The structure factor is proportional to the real part of the dynamic collision frequency and thus strongly dependent on the used interaction, as described in the previous section. With the asymptote (10) follows

$$S(k, \omega \to \infty) \sim \frac{k_B T}{m_e} k^2 \frac{1}{\omega^{15/2}} \tag{15}$$

for a Deutsch-like potential. As is shown in the right graph of figure 3, the simulation data agree well with our analytical expressions.

4. Conclusion

Starting from a generalized linear response theory for the dielectric function we calculate a complex dynamic collision frequency in the long-wavelength limit. The collision frequency is obtained as a force–force correlation function, which we evaluate in different approximations. We combine these approximations in a Gould–DeWitt scheme to account for dynamical screening and strong collisions. We compare our dynamic collision frequency with results obtained by classical MD simulations. Furthermore, we extend our approach to quasi-classical effective interactions, however, neglecting effects of degeneracy and bound state formation. The newly calculated dynamic collision frequencies differ strongly in dependence on the applied potential. A good agreement with MD simulations for a Deutsch-like potential is found. Simulations for the other effective interactions and a classical calculation of the dynamic collision frequency are in progress.

Acknowledgment

This work was supported by the Deutsche Forschungsgemeinschaft (SFB 198 'Kinetik partiell ionisierter Plasmen').

References

[1] Zubarev D N, Morozov V G and Röpke G 1996/97 *Statistical Mechanics of Nonequilibrium Processes* vols 1–2 (Berlin: Akademie Verlag/Wiley)
[2] Röpke G 1998 *Phys. Rev.* E **57** 4673
[3] Röpke G and Wierling A 1998 *Phys. Rev.* E **57** 7075
[4] Reinholz H, Redmer R, Röpke G and Wierling A 2000 *Phys. Rev.* E **62** 5648
[5] Wierling A, Millat Th, Röpke G, Redmer R and Reinholz H 2001 *Phys. Plasmas* **8** 3810
[6] Gould H A and DeWitt H E 1967 *Phys. Rev.* **155** 68
[7] Pfalzner S and Gibbon P 1998 *Phys. Rev.* E **57** 4698
[8] Mermin N D 1970 *Phys. Rev.* B **1** 2362
[9] Selchow A, Röpke G, Wierling A, Reinholz H, Pschiwul T and Zwicknagel G 2001 *Phys. Rev.* E **64** 056410
[10] Röpke G, Selchow A, Wierling A and Reinholz H 1999 *Phys. Lett.* A **260** 365
[11] Kelbg G 1963 *Ann. Phys., Lpz* **12** 219
Deutsch C 1977 *Phys. Lett.* A **60** 317
[12] Zwicknagel G and Pschiwul Th 2002 Private communication
[13] Mahan G D 1990 *Many Particle Physics* (New York: Plenum)
[14] Schmidt P, Zwicknagel G, Reinhard P-G and Toepffer C 1997 *Phys. Rev.* E **56** 7310
Zwicknagel G, Toepffer C and Reinhard P-G 1998 *Phys. Rep.* **309** 117